Available online at www.sciencedirect.com

SciVerse ScienceDirect

Ceramics International 39 (2013) 7115–7118

CERAMICS INTERNATIONAL

www.elsevier.com/locate/ceramint

Synthesis and luminescence properties of Eu^{2+}-doped 8-coordinated SrO phosphors

Keiji Komatsu[a,*], Tomoyuki Shirai[a], Atsushi Nakamura[a,b], Ariyuki Kato[c], Shigeo Ohshio[a], Nobuyoshi Nambu[b], Ikumi Toda[a], Hiroyuki Muramatsu[a], Hidetoshi Saitoh[a]

[a]*Department of Material Science and Technology, Nagaoka University of Technology, 1603-1 Kamitomioka, Nagaoka, Niigata 940-2188, Japan*
[b]*Chubu Chelest Co., Ltd., 3-3-3 Hinagahigashi, Yokkaichi, Mie 510-0886, Japan*
[c]*Department of Electrical Engineering, Nagaoka University of Technology, 1603-1 Kamitomioka, Nagaoka, Niigata 940-2188, Japan*

Received 5 January 2013; received in revised form 18 February 2013; accepted 18 February 2013
Available online 27 February 2013

Abstract

Eu^{2+}-doped SrO (SrO:Eu^{2+}) phosphors were synthesized and their luminescence properties were investigated. Phosphors doped with different Eu^{2+} concentrations were synthesized by the thermal treatment of SrO and Eu powders on a single crystalline MgO substrate at 1500 °C in a reducing atmosphere of Ar and H_2. X-ray diffraction measurements showed that the synthesized phosphors contained 8-coordinated SrO with an orthorhombic crystal system. The phosphors showed a strong blue emission at 456 nm, which was attributed to the Eu^{2+} concentration. In addition, a phosphor doped with 2 at% Eu^{2+} showed an internal quantum efficiency of 30%.

Keywords: Blue phosphor; Strontium oxide (SrO); Luminescence property

1. Introduction

The possibility of using strontium oxide (SrO) as an electrode material has been explored because of its low-driving-voltage discharge property [1–4]. However, several issues hinder the possible applications of SrO; one such issue is its chemical instability in air. Exposed SrO easily reacts with moisture and carbon dioxide present in the air and immediately forms strontium hydroxide ($Sr(OH)_2$) and strontium carbonate ($SrCO_3$), respectively [5].

Recently, we synthesized cesium chloride (CsCl)-type SrO under ordinary pressure by a simple method, which was previously possible only under high pressure (36 GPa) [6,7]. CsCl-type SrO shows fascinating optical and chemical properties because of its crystal structure, containing oxygen with a coordination number of 8, makes it chemically more stable than normal SrO having oxygen with a coordination number of 6.

In this study, we demonstrate the synthesis and luminescence properties of 8-coordinated SrO:Eu^{2+} phosphors. Phosphors doped with different concentrations of Eu^{2+} were synthesized by sintering SrO:Eu powders on a single crystalline MgO substrate in a reducing atmosphere. The crystalline structure of the phosphors was investigated by X-ray diffraction (XRD). In addition, the luminescence properties and internal quantum efficiency of the phosphors were also investigated. Furthermore, we measured the temperature dependence of luminescence properties in the range 50–300 K.

2. Experimental

2.1. Raw materials for the synthesis of SrO:Eu phosphors

Two metal ethylenediaminetetraacetic acid (EDTA) complexes – Sr- and Eu-EDTA – were used for the synthesis of SrO:Eu phosphors. Sr-EDTA and Eu-EDTA solutions were mixed in the ratio [Sr]:[Eu] = $(1-x)$:x, as shown in Table 1. We fabricated five (Sr, Eu)–EDTA complex solutions by varying the molar concentration of Eu (x) from 0.02 to 0.50. These solutions were dried in a spray-dry apparatus (SD-1000, Tokai Rika Kikai Co., Ltd.). The obtained complexes

*Corresponding author. Tel.: +81 258 47 9342; fax: +81 258 47 9300.
E-mail address: Keiji_Komatsu@mst.nagaokaut.ac.jp (K. Komatsu).

0272-8842/$ - see front matter © 2013 Elsevier Ltd and Techna Group S.r.l. All rights reserved.
http://dx.doi.org/10.1016/j.ceramint.2013.02.053

Table 1
List of SrO:Eu raw materials.

Eu concentration (at%)	[Eu]/[Sr] ratio
2	0.02
5	0.05
10	0.1
20	0.2
50	0.5

were then subjected to heat treatment at 800 °C for 3 h to obtain homogeneously mixed raw materials for the synthesis of SrO:Eu^{2+} phosphors.

2.2. Synthesis of SrO:Eu^{2+} phosphors

In order to obtain SrO:Eu^{2+} phosphors, we first mounted the raw materials on a (110) single crystalline MgO substrate ($10 \times 10 \times 0.5\ mm^3$) and subjected it to the thermal treatment in a reducing atmosphere of H_2 and Ar (3 vol%, flow rate: 1 L/min) at 1500 °C in a tube furnace.

2.3. Analysis and evaluation

An X-ray diffractometer (M03XHF MXP3, Mac Science) was used to determine the crystal structure of the phosphors. Their lattice parameters were estimated from the obtained diffraction patterns. Luminance measurements for the phosphor samples were conducted using a luminance meter (LS-100, Konica Minolta Holding, Inc.). The samples were excited by means of a 325-nm He–Cd laser (30 mW; IK3252R-E, Kimmon Koha Co., Ltd.). Internal quantum efficiency of the samples was measured at room temperature by using an integration glass semisphere. The construction details are given in Ref. [8]. The absorbed excitation light and emitted photoluminescence (PL) from the samples or a small piece of opaque quartz as a non-absorbing reference were determined by measuring photomultiplier outputs by means of a band pass filter (Hoya, B390) and a cut-off filter (Toshiba, L42). To investigate the temperature dependence of luminescence of the phosphors in the range 50–300 K, an optical cryostat coupled to a closed-cycle He refrigerator (CryoMini D105 and TCU-4, Iwatani) and the 325-nm line of a He–Cd laser (10 mW; 3056-M-A01, Omnichrome) was used. Details of the PL measurement system are also given in Ref. [8].

3. Results and discussion

3.1. Phase formation and crystal structure

First, the phase formation and crystal structure of the SrO:Eu^{2+} phosphors synthesized with different Eu^{2+} concentrations were investigated. Fig. 1 shows the XRD patterns of Eu^{2+}-doped SrO phosphors with Eu^{2+} concentrations ranging from 2 to 50 at%. The patterns show

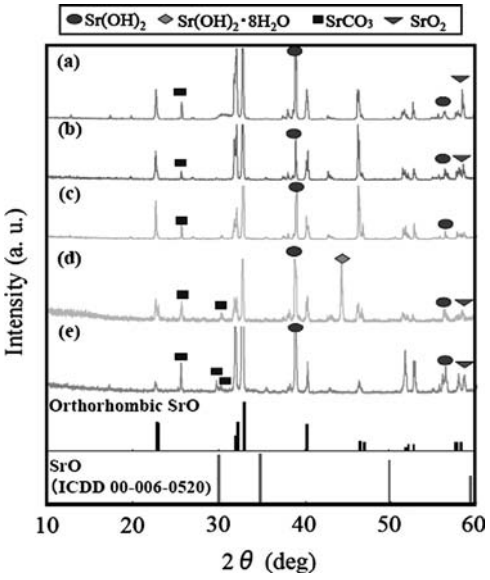

Fig. 1. XRD patterns of SrO:Eu^{2+} phosphors with various Eu^{2+} concentrations: (a) 2 at%, (b) 5 at%, (c) 10 at%, (d) 20 at%, and (e) 50 at%. For comparison, the calculated profiles for orthorhombic SrO and the ICDD card for NaCl-type SrO are also given.

clear differences with increasing Eu^{2+} concentration. All patterns show strong peaks at $2\theta = 25.7°$, 40°, and 56.6°, which were assigned to $SrCO_3$ (021) (ICDD card no. 00-005-0418), $Sr(OH)_2$ (121), and $Sr(OH)_2$ (132) (ICDD card no. 00-027-0847), respectively. The diffraction peak at $2\theta = 59°$ was assigned to SrO_2 (ICDD card no. 00-007-0234). Upon increasing Eu^{2+} concentration from 20 to 50 at%, diffraction peaks corresponding to $SrCO_3$ (002) and (012) at $2\theta = 29.6°$ and 31.5° were observed. It should be noted that none of the obtained XRD patterns matched with any other reported ICDD card. To assign the obtained peaks, we performed theoretical calculations on the basis of their Bragg conditions and periodic interval peaks in the XRD profiles. The crystalline structure identification for the obtained SrO:Eu^{2+} sample was investigated from the agreement with the calculated XRD patterns using traditional various crystalline structures. We attempted to classify the crystalline compounds into three types, namely, rock-salt (NaCl), zinc blende (ZnS), and CsCl types. In case of the SrO powder on MgO, the tetragonally distorted cubic CsCl-type crystal was found [7]. The obtained SrO:Eu^{2+} samples showed good agreement with those for CsCl-type SrO with an orthorhombic lattice. In contrast, the obtained XRD pattern was not matched to NaCl and ZnS type SrO, perfectly. The lattice constants for SrO:Eu^{2+} phosphors with various Eu^{2+} concentrations are listed in Table 2. The calculated c/a values for 2, 5, and 10 at% Eu^{2+}-doped SrO phosphors were almost equal, ranging from about 0.999 to 1.000. When Eu^{2+} concentrations increased above 20 at%, the lattice constants started to decrease. This is ascribed to the relation between the ionic radii of related cations. The Eu^{2+} ions can substitute the host Sr^{2+} ions because

Table 2
Lattice parameters for SrO:Eu^{2+} phosphors with various Eu^{2+} concentrations.

Eu (at%)	Lattice constant			c/a
	a (nm)	*b* (nm)	*c* (nm)	
2	0.3890	0.3932	0.3890	0.9999
5	0.3908	0.3848	0.3906	0.9997
10	0.3911	0.3799	0.3914	1.0008
20	0.3912	0.3805	0.3881	0.9920
50	0.3912	0.3785	0.3893	0.9951

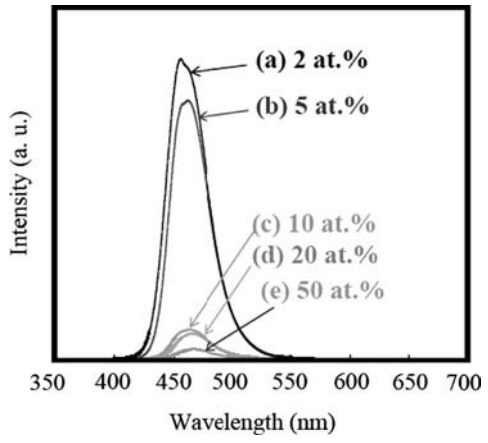

Fig. 2. Photoluminescence spectra for SrO:Eu^{2+} phosphors with various Eu^{2+} concentrations: (a) 2 at%, (b) 5 at%, (c) 10 at%, (d) 20 at%, and (e) 50 at%.

the ionic radius of Eu^{2+} ions (0.1250 nm) is almost equal to that of Sr^{2+} ions (0.1260 nm) [9]. Upon increasing Eu^{2+} concentration, the atomic arrangement of 8-coordinated SrO was changed slightly, as can be seen from Table 2.

3.2. PL of SrO:Eu^{2+} phosphors at various Eu^{2+} concentrations

Fig. 2 shows the PL spectra for SrO:Eu^{2+} phosphors with different Eu^{2+} concentrations (2–50 at%) excited by 325-nm light. We found that the observed PL properties were strongly affected by the Eu^{2+} concentration. For Eu^{2+} concentrations in the range 2–5 at%, strong blue emission peaks were observed at around 456 nm, which indicate the $4f^6 5d^1 \rightarrow 4f^7(^8S_{7/2})$ electric dipole transition of Eu^{2+} ions [10]. We compared the PL intensities obtained at different Eu^{2+} concentrations, as shown in Fig. 3. The emission intensities at 456 nm clearly decreased upon increasing the Eu^{2+} concentration owing to concentration quenching [11]. In our case, the concentration quenching phenomenon was clearly observed and the most efficient Eu^{2+} doping concentration for SrO was 2 at%.

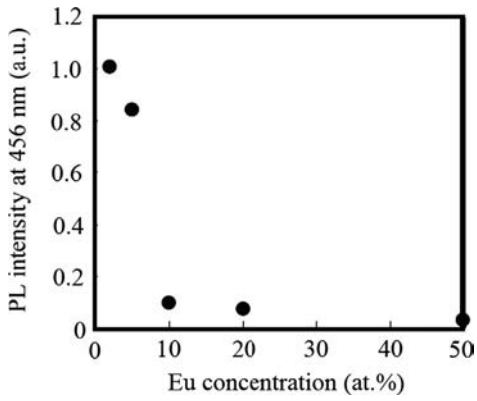

Fig. 3. Dependence of the luminescence intensity on Eu^{2+} concentration in $Sr_{1-x}O:Eu_x^{2+}$ ($x=0.02-0.5$).

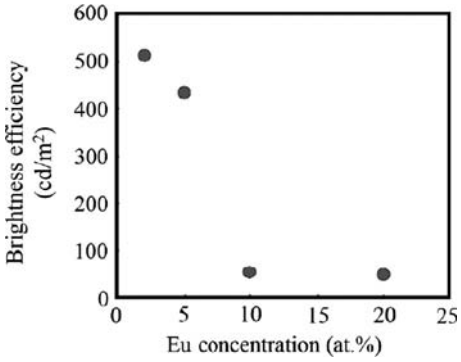

Fig. 4. Relationship between luminance and Eu^{2+} concentration for SrO:Eu^{2+} phosphors.

3.3. Luminance measurements for SrO:Eu^{2+} phosphors at various Eu^{2+} concentrations

Fig. 4 shows the dependence of the luminance of SrO:Eu^{2+} phosphors on the Eu^{2+} concentration. The luminance values were 510, 433, 50, and 44 cd/m^2 for Eu^{2+} concentrations of 2, 5, 10, and 20 at%, respectively. Upon increasing the Eu^{2+} concentration, luminance of the phosphors clearly decreased. The obtained luminance value of 2 at% Eu-doped SrO phosphor was 10 times that of 10 at% Eu-doped SrO phosphor. These phenomena were also concentration quenching of Eu^{2+} ion in the obtained 8-coordinated SrO structure. The highest luminance value was obtained at a Eu^{2+} concentration of 2 at%.

3.4. Quantum efficiency

We measured the internal quantum efficiency of SrO:Eu^{2+} phosphors at an excitation wavelength of 325 nm (Table 3). The quantum efficiencies decreased with increasing Eu^{2+} concentrations. The highest efficiency was 30% at a Eu^{2+} concentration of 2 at%. We believe that this very high efficiency results from a uniform distribution of Eu^{2+} ions in the phosphors.

Table 3
Internal quantum efficiency values for SrO:Eu^{2+} phosphors.

Eu concentration (at%)	Internal quantum efficiency (%)
2	30
5	29
10	7
20	8

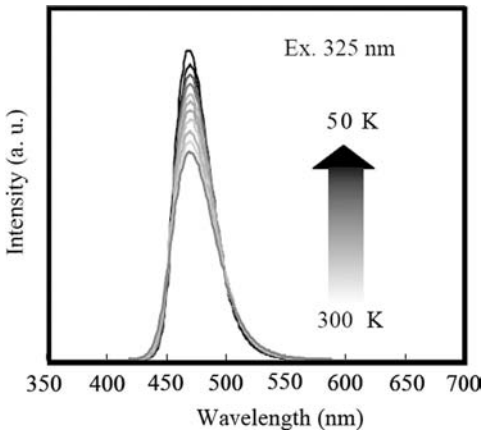

Fig. 5. Temperature dependence of PL spectra for SrO:Eu^{2+} (2 at%) phosphor in the range 50–300 K; the phosphor was excited by 325-nm He–Cd laser.

3.5. Temperature dependence of emission properties

The occurrence of non-radiative process in phosphor materials during low-temperature PL measurements can be reduced [12]. The non-radiative process in phosphor is strongly dependent to its crystal purity. The existence of the normal SrO related materials such as $SrCO_3$ and $Sr(OH)_2$ in the obtained SrO:Eu^{2+} phosphors were confirmed by the XRD analysis. The temperature dependence of the emission properties of a SrO:Eu^{2+} blue phosphor was evaluated to investigate the non-radiative process. The temperature dependence of the emission properties of a SrO phosphor doped with 2 at% Eu^{2+} is shown in Fig. 5. At 300 K, the phosphor exhibited an emission peak corresponding to 456 nm. The position of this emission peak was independent of temperature. The peak intensity at 456 nm increased monotonously with decreasing temperature, as shown in Fig. 6.

4. Conclusions

Eight-coordinated SrO:Eu^{2+} phosphors were synthesized on a (110) single crystalline MgO substrate by the thermal treatment of SrO:Eu powders in a reducing atmosphere. The phosphors showed an intense blue emission peak at

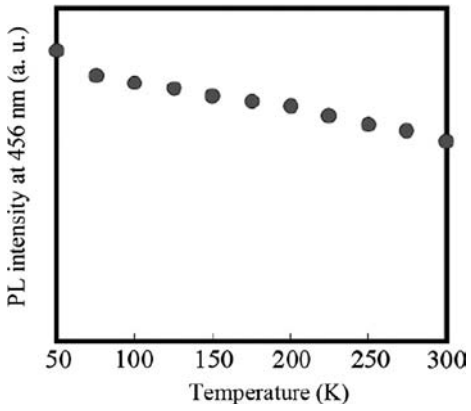

Fig. 6. Relationship between PL intensity at 456 nm and temperature for SrO:Eu^{2+} phosphors.

456 nm. The optimal concentration of Eu^{2+} (2 at%) in SrO was estimated on the basis of concentration quenching. We believe that the synthesized SrO:Eu^{2+} phosphors are promising candidates as blue-light-emitting materials for use in various applications.

References

[1] Y. Shintani, T. Izumi, K. Takagi, M. Inoue, T. Onimaru, S. Kasahara, N. Kosugi, M. Kitagawa, Investigation of conductivity of SrO: high gamma material for protective layer of AC-PDPs, in: SID Symposium Digest of Technical Papers, vol. 42, 2011, pp. 513–515.
[2] H.-Y. Jung, T.-H. Lee, O. Kwon, K.-W. Whan, Address discharge characteristics of high luminous efficacy PDP with SrO protecting layer, in: SID Symposium Digest, vol. 40, 2009, pp. 58–61.
[3] K.-W. Whang, T.-H. Lee, H.-W. Cheong, High luminous efficacy and low-driving-voltage discharges in PDP with SrO–MgO double protecting layer, in: SID Symposium Digest, vol. 41, 2010, pp. 732–734.
[4] H. Uchiike, K. Sekiya, T. Hashimoto, T. Shinoda, Y. Fukushima, Optimum composition of CaO, SrO dielectric materials in AC plasma display panels, IEEE Transactions on Electron Devices 30 (1983) 1735–1742.
[5] Kagaku Daijiten, Kyoritsu Shuppan Co., Ltd., (in Japanese).
[6] Y. Sato, R. Jeanloz, Phase transition in SrO, Journal of Geophysical Research 86 (1981) 11773–11778.
[7] K. Komatsu, H. Akasaka, A. Nakamura, S. Ohshio, N. Nambu, I. Toda, H. Saitoh, High pressure SrO synthesized from Sr–O powder mounted on single crystal MgO at normal pressures, Journal of Physics and Chemistry of Solids, unpublished results.
[8] A. Kato, M. Yamazaki, H. Najafov, K. Iwai, A. Bayramov, C. Hidaka, T. Takizawa, S. Iida, Radiative and non-radiative processes of Ce related transitions in $CaGa_2S_4$ and $SrGa_2S_4$, Journal of Physics and Chemistry of Solids 64 (2003) 1511–1517.
[9] R.D. Shannon, Revised effective ionic radii and systematic studies of interatomic distances in halides and chalcogenides, Acta Crystallographica A32 (1976) 751.
[10] Phosphor Handbook, CRC Press, pp. 192–193.
[11] D.L. Dexter, J.H. Schlman, Journal of Chemical Physics 22 (1954) 1063.
[12] K. Komatsu, A. Nakamura, A. Kato, S. Ohshio, H. Akasaka, H. Saitoh, Investigation of temperature dependence on emission properties of Sr–Al–O:Eu^{2+} phosphor synthesized using elemental diffusion from substrate, Materials Science and Engineering 18 (2011) 102017.